

# Development of an *In Vitro* PIV Setup for Preliminary Investigation of the Effects of Aortic Compliance on Flow Patterns and Hemodynamics

MARTIN BÜSEN, CHRISTIAN ARENZ, MICHAEL NEIDLIN, SAM LIAO, THOMAS SCHMITZ-RODE,  
ULRICH STEINSEIFER, and SIMON J. SONNTAG

Department of Cardiovascular Engineering, Institute of Applied Medical Engineering, Helmholtz Institute, RWTH Aachen University, Aachen, Germany

(Received 10 January 2017; accepted 23 May 2017; published online 8 June 2017)

Associate Editors Hwa Liang Leo and Ajit P. Yoganathan oversaw the review of this article.

**Abstract**—The aorta with its compliance plays a major role in hemodynamics as it saves a portion of ejected blood during systole which is then released in diastole. The aortic compliance decreases with increasing age, which is related to several cardiovascular imparities and diseases. Changes in flow patterns and pressure curves, due to varying aortic compliance, are difficult to investigate *in vivo*. As a result, the aim of the present work was to develop an *in vitro* setup enabling standardized investigations on the effect of compliance changes on flow patterns and pressure curves. Therefore an experimental setup with an anatomically correct silicone phantom of the aortic arch was developed, suitable for optical flow measurements under pulsatile inflow conditions. The setup was developed for precise adjustments of different compliances and optical flow measurements. Particle image velocimetry measurements were carried out downstream of the aortic valve in the center plane perpendicular to the valve with compliance adjusted between  $0.62 \times 10^{-3}$  to  $1.82 \times 10^{-3} \text{ mmHg}^{-1}$ . Preliminary results of the *in vitro* investigations showed that decreases in compliance results in significant increases in pressure changes with respect to time ( $dp/dt$ ) and altered pressure curves in the aortic arch. In terms of flow, an increased aortic stiffness lead to higher mean velocities and decreased vortex development in the aortic sinuses. As *in vivo* validation and translation remains difficult, the results have to be considered as preliminary *in vitro* insights into the mechanisms of (age-related) compliance changes.

**Keywords**—Aortic compliance, Aortic flow, Hemodynamics, Particle image velocimetry.

## ABBREVIATIONS

LDV	Laser Doppler velocimetry
MR	Magnetic resonance
Nd:Ylf	Neodymium-doped yttrium lithium fluoride
PIV	Particle image velocimetry
PTV	Particle tracking velocimetry
US	Ultra sound

## SYMBOLS

$A$	Area ( $\text{cm}^2$ )
$C$	Compliance ( $\text{mmHg}^{-1}$ )
$dp/dt$	Pressure change with respect to time ( $\text{mmHg s}^{-1}$ )
$\eta$	Dynamic viscosity ( $\text{Pa s}$ )
$n$	Refractive index
$\rho$	Density ( $\text{kg m}^{-3}$ )
$m$	Mass (kg)
$p$	Pressure (mmHg)
$v$	Velocity ( $\text{cm s}^{-1}$ )
$T$	Temperature ( $^{\circ}\text{C}$ )

## INTRODUCTION

The aorta plays an important role in the cardiovascular system. One major mechanical characteristic is the physiological compliance, leading to the Windkessel effect: due to the elastic vessel walls, the systolic pressure leads to an expansion of the aorta and a part of the ejected stroke volume is stored. This blood volume is dispensed during diastole, sustaining dias-

Address correspondence to Martin Büsen, Department of Cardiovascular Engineering, Institute of Applied Medical Engineering, Helmholtz Institute, RWTH Aachen University, Aachen, Germany. Electronic mail: buesen@ame.rwth-aachen.de

tolic pressure in the cardiovascular system and contributing to organ and coronary perfusion.<sup>3,4</sup> Aortic compliance is dependent on different factors but generally decreases with age, except in the period between birth and early childhood, where it is increasing.<sup>16</sup> Changes in compliance can affect hemodynamics, such as systolic and diastolic pressures, pulse wave velocity, and systolic blood velocities.<sup>4,18</sup> Those changes are related to several cardiovascular imparities and diseases, like hypertension or heart failure, but the mechanisms are not completely understood.<sup>8,12,19,21</sup>

One problem lies in the difficulty to investigate the influence of compliance changes on flow patterns and hemodynamics *in vivo*. Firstly, controlled isolated compliance changes are hard to perform. Drugs can be applied but it can influence the entire cardiovascular system. Alternatively, the native aorta can be replaced by a stiffer graft,<sup>13</sup> which is a complex procedure. Secondly, *in vivo* flow investigations techniques, such as Doppler ultrasound (US) or magnet resonance imaging (MRI), are limited to their spatial and temporal resolution. Thirdly, parameters that influence hemodynamics can interact (i.e., compliance, pulse wave velocity, systolic pressures, heart work), making it difficult to investigate the effects separately.<sup>13</sup> In this case, *in vitro* methods are appropriate tools, as they offer the opportunity to standardize investigations. For example Keshavarz-Motamed *et al.* published two studies including a mock circulation loop with a realistic aortic compliant model.<sup>14,15</sup> The manufactured aortic model had a compliance comparable to a human aorta and compliance adjustments were made by putting rigid ring structures around the model.

In order to investigate aortic flow patterns *in vitro*, optical measurement techniques are favorable, as they offer a good spatial and temporal resolution. Examples of optical flow measurement techniques used for assessment of aortic flows include particle image velocimetry (PIV),<sup>6</sup> laser Doppler velocimetry (LDV)<sup>17</sup> or particle tracking velocimetry (PTV).<sup>9</sup> In order to provide good optical access without distortion, the vessel models must be transparent and usually needs to have planar windows, which is often made by silicone casts in the form of a block.<sup>7,25</sup> Although these requirements are hard to combine with elastic properties, a few studies can be found where optical flow measurements were carried out while considering aortic elasticity. Gülan *et al.* investigated the influence of a stiff and flexible silicone aorta on flow and hemodynamics with means of particle tracking.<sup>10</sup> In a study by Yip *et al.*, a compliant model of a human aorta was manufactured to validate the results of numerical simulations concerning wall shear stress distributions.<sup>26</sup> Quantitative data for the compliance was not provided in both works and compliance changes was

not performed. Examples of more fundamental work in which elastic silicone tubes have been used include studies by Pielhop *et al.*<sup>23</sup> and Burgmann *et al.*<sup>5</sup> They investigated an oscillating flow in an elastic 180° curved tube and a straight tube, respectively.

The purpose of this work was twofold: (1) to develop an experimental setup of an anatomically correct aortic arch with an adjustable compliance in the range of physiological values, which is suitable for optical flow measurements, and (2) to perform first investigations on the effect of (age-related) compliance changes on flow patterns and hemodynamics *in vitro* with means of PIV.

## MATERIALS AND METHODS

A transparent silicone model of the aortic arch was manufactured, which was surrounded by a fluid compartment. This enabled fulfillment of the requirements of having a non-distorted optical access and allowed compliance adjustments with an attached compliance chamber. The aortic model was connected to a mock circulation loop mimicking native heart pulsatility with subsequent PIV measurements being taken. In this section, details about the manufacturing, experimental setup, measurements and post processing are given.

### *Manufacturing of the Silicone Aorta*

The aortic geometry of a healthy adult human volunteer (male 33 years) was extracted from magnetic resonance (MR) data using Mimics (Materialise, Leuven, Belgium). The geometry was used to design a mold in 3-matic (Materialise, Leuven, Belgium). The inner wall of the mold represented the outer wall of the original vessel. The mold was manufactured with a 3D printer (Eden 350V, Objet Geometries Ltd., Israel). The mold and four cross sections are shown in Fig. 1. For the molding process, firstly, the inner surface of the hollow mold was covered with polyvinyl alcohol. A two component silicone (Elastosil RT620, Wacker, Germany) was mixed and degassed. This silicone is highly elastic and has a low viscosity after mixing which is advantageous for the manufacturing process (mechanical properties of silicone see Table 1). To fill the entire inner surface of the mold, 35 mL of silicone was used. During the curing process, the mold was mounted to a rotating mandrel and was rotated for 30 min to ensure an even distribution of silicone on the surface. Two additional layers of silicone were applied the same way to guarantee complete coverage of the inner surface and provide sufficient wall thickness. Based on CAD data, it was theoretically calculated that each layer (35 mL silicone) would be 0.5 mm thick

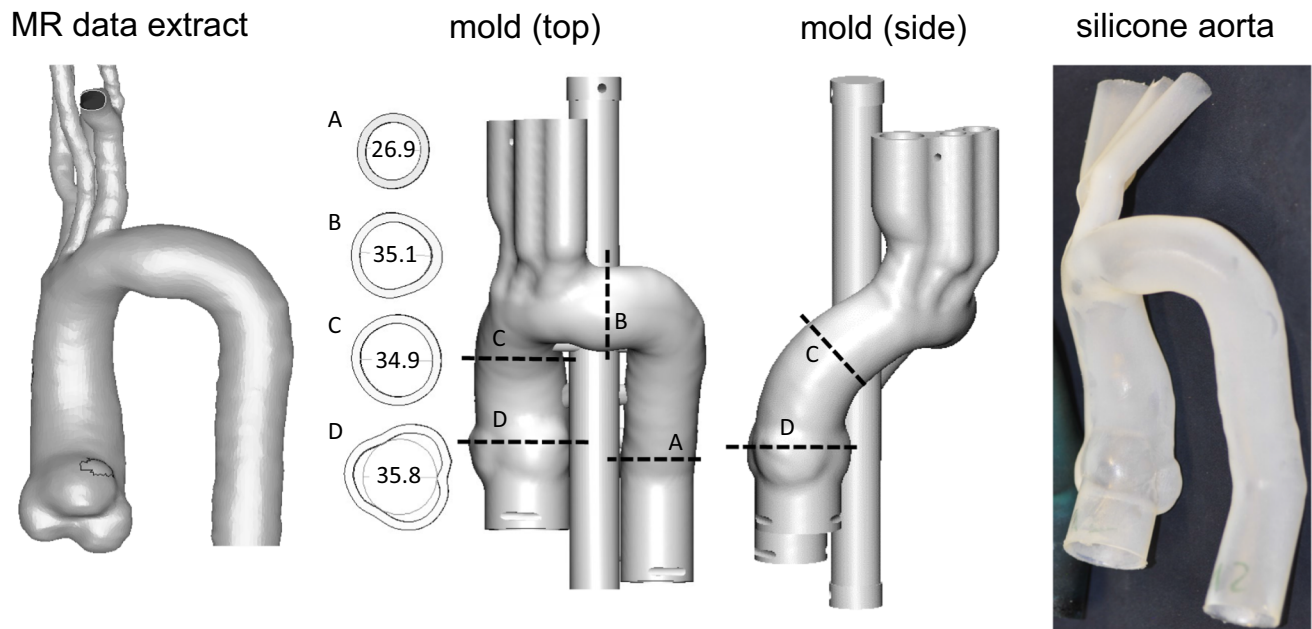


**FIGURE 1.** Left: MR-Data extract executed with Mimics (Materialise, Belgium), middle: CAD image of the mold which was 3D-printed (top and side view) and four cross sections, right: image of the manufactured silicone aorta.

**TABLE 1.** Properties of silicone RT 620.

Hardness shore A	17
Tensile strength ( $\text{N mm}^{-2}$ )	5
Elongation at break (%)	900
Tear strength ( $\text{N mm}^{-2}$ )	12

resulting in a final wall thickness of 1.5 mm. This value was chosen as a compromise to fulfill the two requirements: mechanical stability to avoid cracks and optical accessibility. Due to manufacturing tolerances, the thickness had an error of  $\pm 0.5$  mm. After the curing process, the silicone model was removed from the mold. The high elasticity of the silicone was advantageous to demolding, which was considered during the initial design. The resultant silicone model of the aorta is shown in Fig. 1.

### Compartment

In order to provide optical access for the PIV measurements and allow adjustment of the aortic compliance, a compartment ( $22 \times 27 \times 16$  cm) was used to surround the silicone aorta (Fig. 2). The compartment was filled with a water glycerol mixture of 56.6%/43.4% ( $m_{\text{Gl}}/m_{\text{w}}$ ) to match the refractive index of the silicone aorta ( $n \approx 1.402$ ) at  $45^\circ\text{C}$ . Both sidewalls and the top plate were made of acrylic glass to ensure optical access for both the camera and laser. The top plate was fixed with screws to allow opening of the compartment. Connection of a mock circulation

loop to the aortic arch was made possible by using custom designed connectors to seal the compartment. The silicone phantom was mounted to an inlet tube with a bileaflet mechanical heart valve (SJM Regent 25 mm, St.Jude Medical Inc., USA), which was positioned in an anatomically correct location. A compliance chamber with an adjustable air volume was connected to the compartment. It was possible to adjust the aortic compliance with this attached chamber, as the trapped air was the only compressible fluid within the system (Fig. 2): aortic expansion leads to compression of air volume. By changing the air volume, different compliances can be achieved. The compliance chamber had a total fill volume of  $\sim 2.28$  L (diameter = 11 cm, height = 24 cm). Air volumes for the different compliances are given in Table 2.

### Experimental Setup

The mock circulation loop (Fig. 3) consisted of two fluid columns with a diameter of 45 mm to represent the atrium and ventricle, separated by a mechanical valve (AlSCO, Lithia Springs, USA), modeling the mitral valve. Contractility of the ventricle was provided using air pressure produced by a Medos driving system (Medos AG, Germany, Stolberg). This system is normally used for pulsatile ventricular assist devices, where the air pressure drives the movement of a membrane. The system was run at 65 bpm. The resultant pressure curve in the ventricle is shown in Fig. 3. The ventricle was connected to the inlet of the

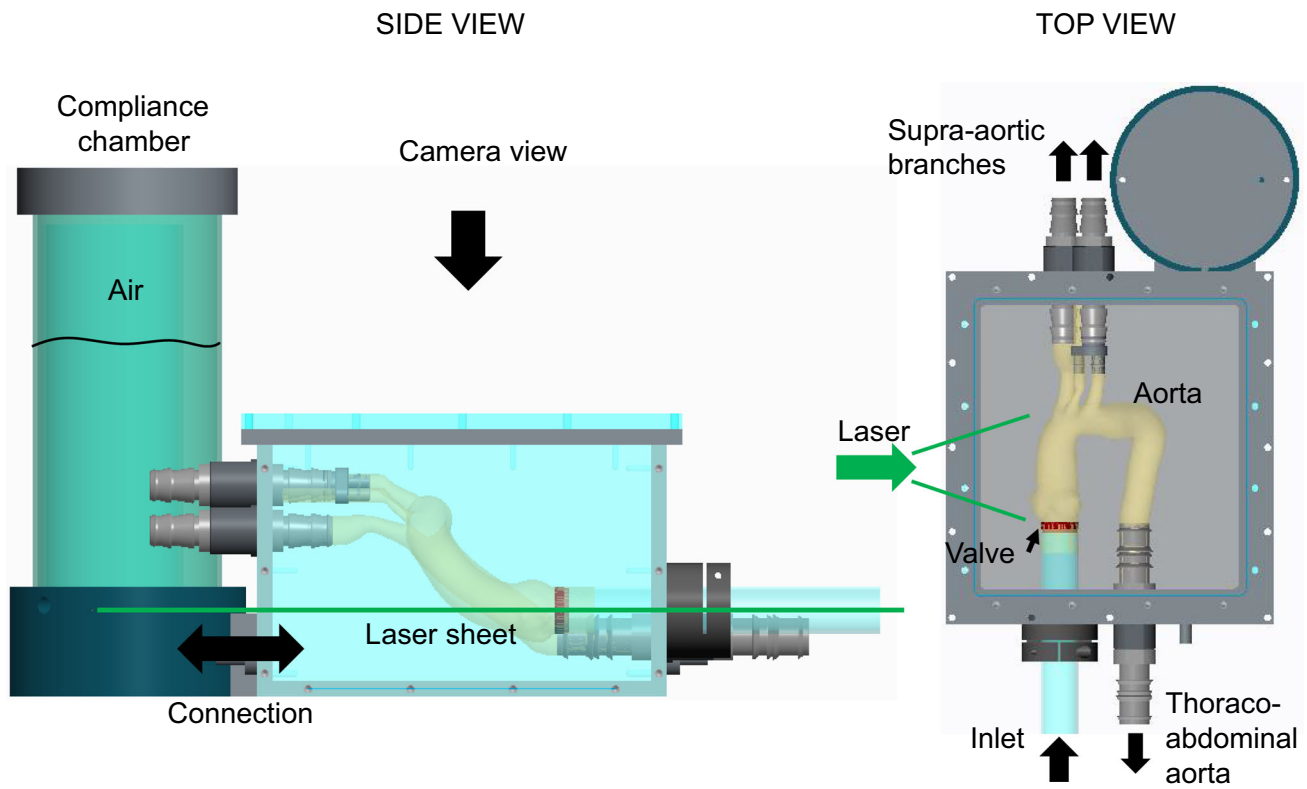


FIGURE 2. Experimental setup of the aortic model in the compartment with the attached compliance chamber, used to adjust aortic compliance. Left: side view, right: top view.

TABLE 2. Compliance adjustments.

Setup	$A_{min}$ (cm <sup>2</sup> )	$A_{max}$ (cm <sup>2</sup> )	$\Delta p$ (mmHg)	$V_{air}$ (dm <sup>3</sup> )	$C$ (x10 <sup>-3</sup> mmHg <sup>-1</sup> )	$Q$ (L min <sup>-1</sup> )
1 (max)	8.3	9.1	53	0.65	1.82	2.81
2	8.1	8.7	61	0.41	1.21	2.75
3 (min)	7.9	8.25	72	0	0.62	2.63

$A_{min}$  minimum area measured during pump cycle,  $A_{max}$  maximum area measured during pump cycle,  $\Delta p$  according pressure difference for  $A_{max}$  and  $A_{min}$ ,  $V_{air}$  volume of air in the compliance chamber,  $C$  determined compliance,  $Q$  mean flow (cardiac output).

compartment, which contained the silicone aorta. The outgoing tubes of the compartment were connected to the atrium. The loop was filled with the same water glycerol mixture used to fill the compartment ( $m_{GI} = 56.6\%$ ). A temperature of  $T = 45 (\pm 1) ^\circ\text{C}$  was maintained with a heating circuit connected to the compartment. The fluid viscosity at  $45 ^\circ\text{C}$  was measured and found to be  $\eta = 3.6 (\pm 0.1) \text{ mPa s}$  (AMVn, Anton Paar, Austria), mimicking blood viscosity for high shear rates,<sup>11</sup> which is common practice, as the nonlinear viscosity of blood is difficult to model.<sup>20</sup> The average flow was measured with a clamp-on US flow probe in the tube leading to the column representing the left atrium (SonoTT, Emtec, Germany). Pulsatile inflow (ventricle to aorta) flow measurements were not

feasible, as the flow probe would have required a longer inlet section, which was kept as short as possible to avoid inertial effects. Pressure was measured in the aortic arch ( $p_{aorta}$ ), compartment ( $p_{comp}$ ) and ventricle ( $p_{vent}$ ) (DPT-6000, Codan pvb, Germany), see Fig. 3. The signals were monitored and recorded with a data acquisition system (CompactDAQ, National Instruments, USA).

A high speed camera (X3, IDT, USA) with an AF Micro-Nikkor 60/F2.8D objective (Nikon Inc., USA) was positioned with a top view of the box. A pulsed laser beam (Nd:Ylf-Laser, Pegasus, NewWave Research Inc., USA) entered a light sheet optics. The resultant laser light sheet, thickness of  $\sim 0.8 \text{ mm}$ , entered the box perpendicular to the side wall in hori-

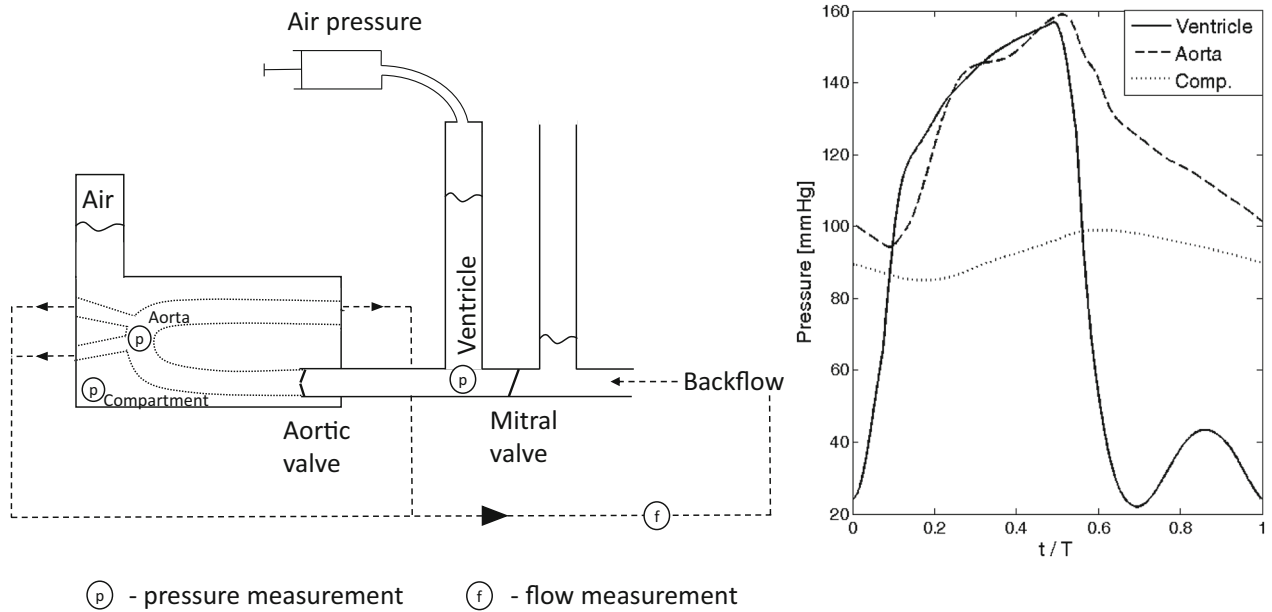


**FIGURE 3.** Schematic view of the experimental circuit (left) and according pressure curves of compliance setup 1 for one cycle in the aortic model, in the ventricle and in the compartment (right).

zonal alignment (Fig. 2). The laser illuminated fluid suspended fluorescent particles with a diameter of  $10\ \mu\text{m}$  (microParticles GmbH, Germany,  $\rho = 1.06\ \text{g cm}^{-3}$ ). The laser sheet was in-line with the center plane perpendicular to the aortic valve (Fig. 2).

#### PIV Measurements & Post Processing

Image acquisition was carried out with Dynamic Studio (Dantec Dynamics, Denmark). Aortic compliance was adjusted three times and PIV measurements were taken for each compliance (Table 2). Ten cycles were recorded with a resolution of 120 image pairs per cycle. As the system ran at 65 bpm the resulting recording rate was 130 Hz. The time delay ( $dt$ ) between the image pairs was set up to be  $500\ \mu\text{s}$ , achieving a maximum particle displacement of about  $\frac{1}{4}$  of the interrogation area size for the highest appearing velocities.<sup>24</sup> The field of view was  $68 \times 54\ \text{mm}$ . The final resolution was  $54\ \mu\text{m}/\text{pixel}$ .

Post processing of the particle images consisted of two parts: the determination of (1) the compliance and (2) the velocity fields. Compliance was determined by analyzing the images for edges with a Canny edge detecting algorithm (MATLAB, Mathworks, USA), which identified the inner aortic walls in a small region 20 mm distal from the aortic valve. As the inner walls were determined in the mid plane their distance was used to calculate the cross sectional area of the silicone aorta (Fig. 4). Calibration of optic scaling was done with a rigid tube of a known and fix diameter, to which the silicone aorta was attached (Fig. 2). Simultaneous

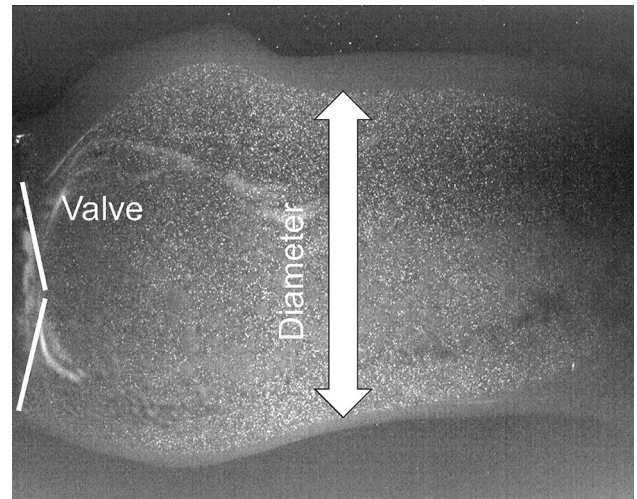


**FIGURE 4.** Particle image with schematic diameter detection.

pressure recordings,  $p_{\text{aorta}}$  (inside the aorta) and  $p_{\text{comp}}$  (outside the aorta), were used to calculate transmural pressure (Eq. 1),  $p_{\text{trans}}$ , which is responsible for aortic expansion.

$$p_{\text{trans}} = p_{\text{aorta}} - p_{\text{comp}}. \quad (1)$$

Physiologically,  $p_{\text{comp}} \approx 0\ \text{mmHg}$ , as this is the pressure in the surrounding tissue. In terms of compliance, different clinical definitions can be found. They are summarized by O'Rourke *et al.*<sup>22</sup> In the present work, the compliance was determined based on

diameter changes and corresponding pressure changes during the simulated cardiac cycle, as described by Laogun and Gosling<sup>16</sup> and Burgmann *et al.*<sup>5</sup> The change in pressure,  $\Delta p$ , and the resulting change in the cross section area,  $\Delta A$ , related to the minimum measured area  $A_{\min}$  were used to calculate the compliance,  $C$ , as shown (Eq. 2).

$$C = \frac{1}{\Delta p} \times \frac{\Delta A}{A_{\min}} [\text{mmHg}^{-1}], \quad (2)$$

Other (clinical) definitions for compliance, for example, is without normalization to  $A_{\min}$ , calculated as  $C = \Delta A / \Delta p$  ( $\text{mm}^2 \text{mmHg}^{-1}$ ). Another definition is the total arterial compliance (“area method”), which is calculated based on the heart stroke volume and resultant pressure differences in the aorta, resulting in units of ( $\text{mL mmHg}^{-1}$ ).<sup>22</sup>

For PIV post processing, recorded images were analyzed with Dynamic Studio (Dantec Dynamics, Denmark). An adaptive correlation with a final interrogation area size of  $32 \times 32$  pixels with an overlap of 50% was applied. The resulting vector fields of 10 cycles were averaged, generating 120 averaged velocity fields for one cycle. The final resolution of the vector field was  $0.84 \times 0.84$  mm.

## RESULTS

In this section the results for the compliance measurements are presented; and a comparison of aortic pressure curves, pressure changes with respect to time ( $dp/dt$ ) and vector fields for different compliances are presented.

### Compliance

Three different compliance values have been adjusted by changing the amount of air in the compliance chamber. In Fig. 5, the post processed cross sectional area was plotted against the corresponding transmural pressure for the two exemplarily compliances  $C_1$  (max) and  $C_3$  (min). Detailed values (area, amount of air, pressure difference) for all setups are given in Table 2. The maximum area was  $9.1 \text{ cm}^2$  for the most flexible setup ( $C_1$ ) and  $8.25 \text{ cm}^2$  for the stiffest setup ( $C_3$ ), the minimum area was  $8.3$  and  $7.9 \text{ cm}^2$ , respectively. The according pressure differences for maximum and minimum area were  $53 \text{ mmHg}$  (most flexible setup) and  $72 \text{ mmHg}$  (stiffest setup). Using Eq. (2), the obtained compliances had values of  $C_1 = 1.82 \times 10^{-3} \text{ mmHg}^{-1}$  and  $C_3 = 0.62 \times 10^{-3} \text{ mmHg}^{-1}$ , which was a decrease of about 63%. The decrease in maximum area was about 7%.

### Pressure and ( $dp/dt$ ) Curves

In Fig. 6, the aortic pressure and ( $dp/dt$ ) curves are shown for the three compliance adjustments. The pressure within the ventricle did not significantly change with changes in compliance, therefore only one ventricle pressure curve was plotted for orientation. The results show that the pressure pulsatility was attenuated for higher compliances. The systolic pressure did not increase but the diastolic pressure decreased with a stiffer aortic setup by about  $20 \text{ mmHg}$  for  $C_{\max} - C_{\min}$ . Also, the increase of pressure was faster in case of the stiffer aorta, which can be quantified with the ( $dp/dt$ ) curves, shown in Fig. 6. Evaluating the ( $dp/dt$ ) curves, it was found that with a stiffer aorta the maximum pressure change with respect to time increased from  $450 \text{ mmHg s}^{-1}$  for  $C_1(\text{max})$  to  $1000 \text{ mmHg s}^{-1}$  for  $C_3(\text{min})$ , which corresponds to an increase of 122%.

### Flow Fields

The flow fields downstream of the aortic valve in the center plane perpendicular to the valve for three compliances are shown in Fig. 7 for different time points after valve opening (time points A–E are marked in the ventricular pressure curve). The overall flow pattern was similar for every compliance adjustment: In the early ejection phase, the fluid was accelerated (A), hereafter a central jet could be observed (B + C), followed by valve closure and tension release of the silicone aorta, which was accompanied by vortex development in the aortic root (D) and lower velocities in diastole (E). Comparing the flow fields for the different compliances, it can be noted, that the velocities in early ejection phase (A) were higher for the stiffer aorta. Here, the mean velocity in the measurement plane is about  $0.18 \text{ cm/s}$  for most flexible setup ( $C_1$ ) and  $0.28 \text{ cm/s}$  in case of the stiffer aorta ( $C_3$ ), which is an increase of about 56%. At this specific time point areas are  $8.8 \text{ cm}^2$  ( $C_1$ ) and  $8.17 \text{ cm}^2$  ( $C_3$ ). Also, the vortices developing in the sinuses were less significant with decreasing compliance during systole and diastole (C + D). Shortly after valve closing (D) it can be seen, that the backflow towards the valve was lower in case of the stiffer aorta.

## DISCUSSION

In this work, an aortic model setup with adjustable compliance was developed and optical PIV flow measurements were performed downstream of the aortic valve in the center plane perpendicular to the valve. The aim was to develop an experimental setup

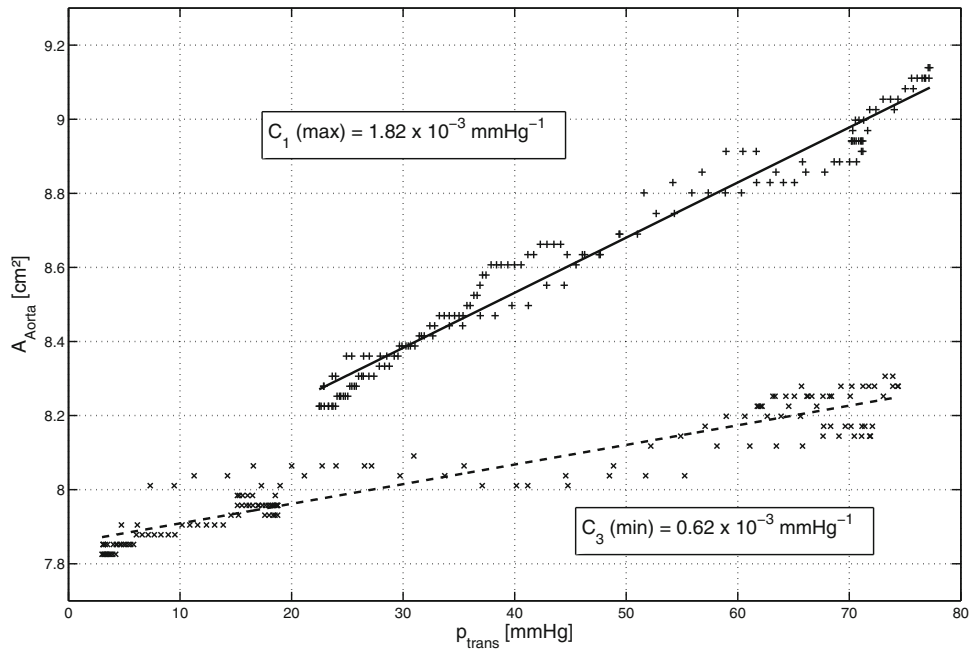


**FIGURE 5.** Aortic area (calculated based on the diameter) against transmural pressure. Data with linear fit is shown for setup 1 (maximum compliance) and setup 3 (minimum compliance).

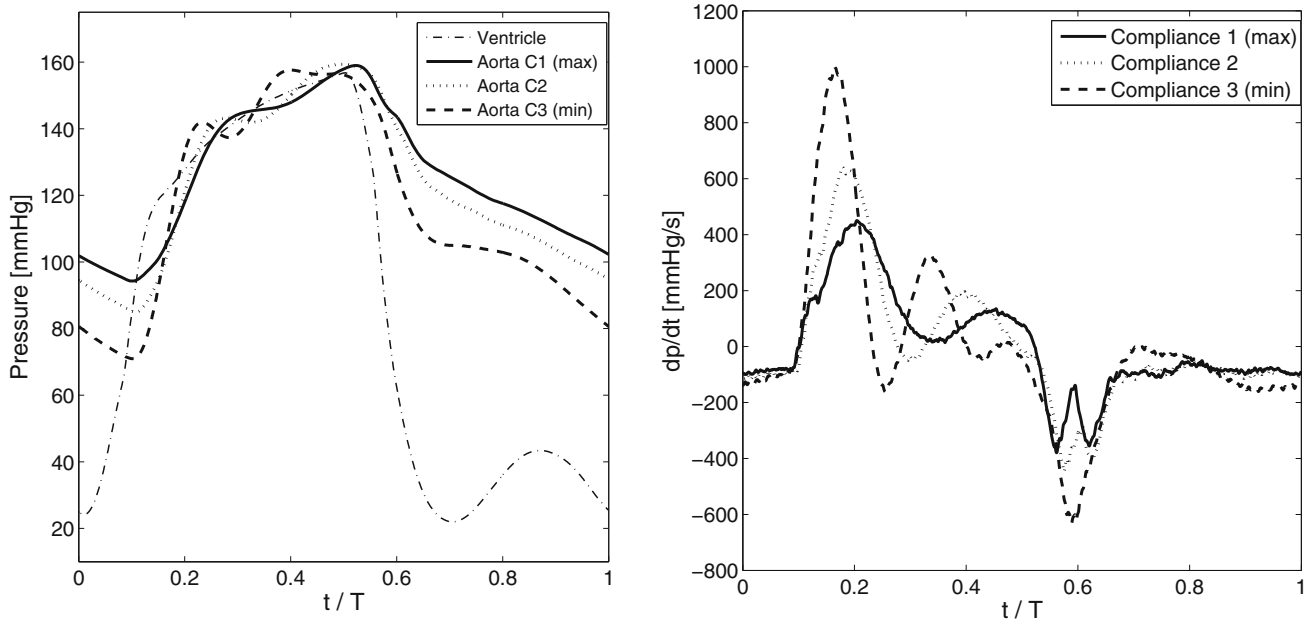


**FIGURE 6.** Left: Aortic pressure for compliance setups 1–3; Right: pressure change with respect to time ( $dp/dt$ ) for compliance setups 1–3.

which allowed for optical flow measurements and fast and easy compliance adjustments to enable investigations of compliance changes in a standardized manner, which is hardly feasible *in vivo*. With this setup, different compliances were adjusted and determined, and the effects on flow and pressure curves were investigated *in vitro*. To the best of our knowledge, this is the first

time that optical flow measurements in a model of the aortic arch in combination with different compliance adjustments (and determination) has been carried out.

Compliance was adjusted between  $0.62$  to  $1.82 \times 10^{-3} \text{ mmHg}^{-1}$ . According to Laogun and Gosling, this corresponds to aortic compliances in humans between the ages of 15–65 years.<sup>16</sup> However,

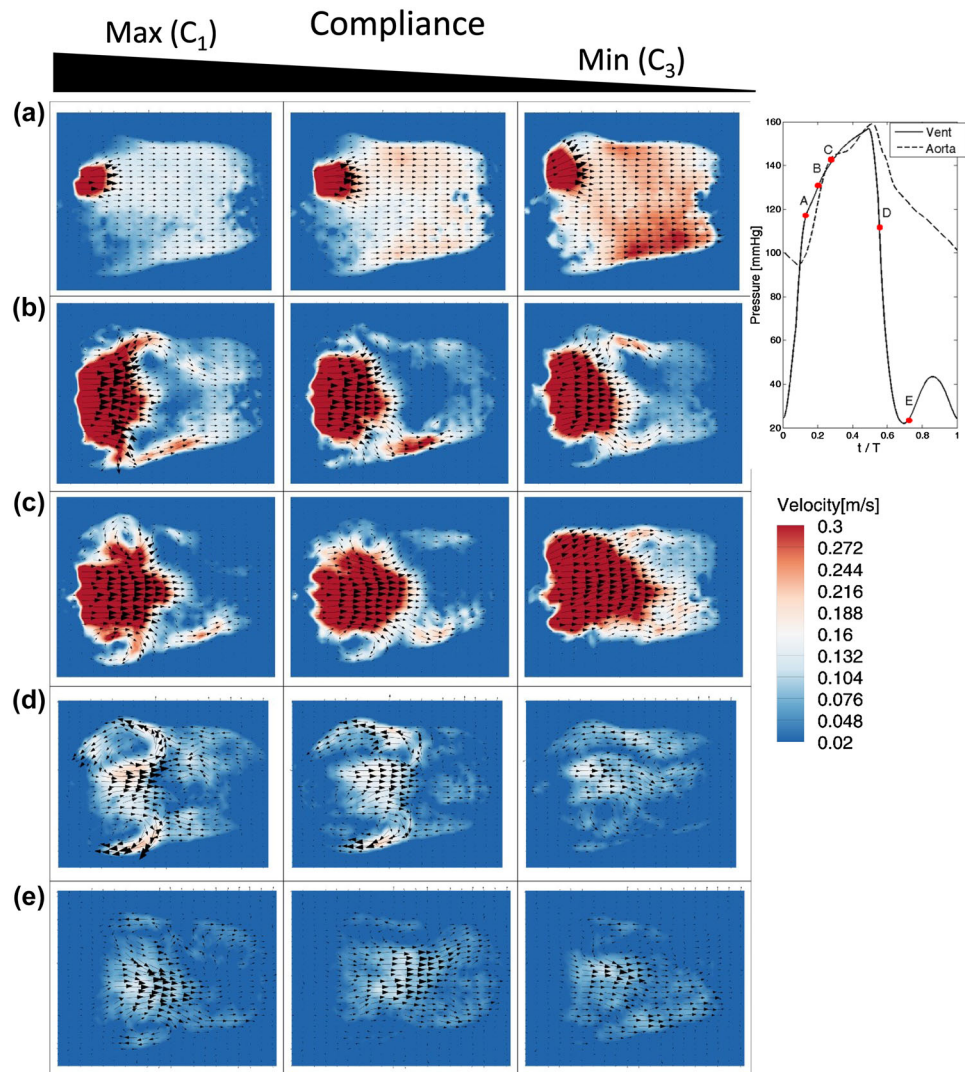


**FIGURE 7.** Flow fields for specific time points (A–E) downstream of the aortic valve in the center plane perpendicular to the valve for one pump cycle (systole and diastole) on base of data for compliance setup 1–3. Markers indicate the time points (A–E) in the pressure curve.

there are different clinical studies which report other values, summarized by O'Rourke *et al.*<sup>22</sup> The compliance changes could be easily achieved by changes of air and water volumes in the compliance chamber. This setup facilitates the comparison of the data acquired for different compliances as no further modification is required, in contrast to using different aortic phantoms with different mechanical properties, where reassembling, recalibration and readjustment of the whole system would become necessary. However, the modeling of the aortic compliance in the presented manner is technically controlled by both the mechanical properties of the aortic silicone model and the amount of air in the compliance chamber. This results in changes in pressure around the aortic model (“surrounding tissue”).

The collected data for different compliances shows that a decrease of 63% in aortic compliance leads to a

significant increase of 122% in the aortic pressure change with respect to time ( $dp/dt$ ). Regarding the impact of changed compliance to flow patterns downstream of the aortic valve, the comparison shows that mean velocities in early systole are higher for decreasing elasticity in the range of about 56%. One reason is the decrease in maximum area, but it is only about 7%; another reason might be the fact that less fluid volume is stored in the expanded part of the silicone aorta and the pressure change with respect to time is higher in the case of a stiffer aorta. These findings confirm the qualitative findings reported by Gülan *et al.*<sup>10</sup> Secondly, vortex development in the aortic sinuses were less significant, which could also be caused by the less expanding vessel walls. Vortex formation in the aortic sinuses is important in terms of coronary perfusion, washout and leaflet closure.<sup>3</sup> The overall flow pattern



of the mechanical valve were in good agreement to those measured in other flow studies of mechanical heart valves,<sup>1,2</sup> although quantitative differences were observable due to the diminished cardiac output. In detail, this was the acceleration phase accompanied by a central jet, the peak flow phase and the deceleration phase accompanied by a backflow and vortex development in the aortic sinuses.<sup>1,2</sup>

Compared to the *in vivo* situation, the mock circulation loop showed some discrepancies, including lower average flow (cardiac output), higher systolic pressures and a longer systolic peak. The native aortic valve has been modeled with a bileaflet mechanical valve, leading to altered flow patterns (except in patients with this kind of heart valve prostheses). A biological valve (trileaflet valve) was not used, as the applied fluid would have damaged the valve. Future work will be carried out to optimize the mock circulation loop; however, it is challenging to perfectly mimic *in vivo* conditions, while fulfilling certain requirements (i.e., measurement technique). Thus, a quantitative translation of the results to *in vivo* should be carried out with consideration of these limitations. Besides, physiological hemodynamics are influenced by auto regulation mechanisms, adaption of heart work to the physiologic situation, or changes in the mechanical characteristics of the vessel (i.e., vasodilation/vasoconstriction). For example, a decreased diastolic pressure would be regulated by the circulatory system, leading to higher systolic pressure levels. However, the focus of this study was (1) to present an experimental setup allowing for isolated investigations of effects of aortic compliance changes and (2) to perform first comparative examinations.

In conclusion, an *in vitro* setup of an anatomic correct silicone aortic arch with an adjustable compliance is presented, which allows for effective compliance changes in physiological ranges in a standardized manner while allowing PIV flow measurements in the aortic arch. Investigations on the effect of compliance changes show that decreased compliance results in increased peak velocities and pressure changes with respect to time, as well as altered pressure curves and decreased vortex formation in the aortic sinuses. As an *in vivo* validation and translation remains difficult, the results have to be considered as preliminary *in vitro* insights into the mechanisms of (age-related) compliance changes.

#### CONFLICT OF INTEREST

Martin Büsen, Christian Arenz, Michael Neidlin, Sam Liao, Thomas Schmitz-Rode, Ulrich Steinseifer

and Simon Sonntag declare that they have no conflict of interest.

#### ETHICAL APPROVAL

This article does not contain any studies with human participants or animals performed by any of the authors.

#### REFERENCES

- <sup>1</sup>Akutsu, T., and A. Matsumoto. Influence of three mechanical bileaflet prosthetic valve designs on the three-dimensional flow field inside a simulated aorta. *J. Artif. Organs* 13:207–217, 2010.
- <sup>2</sup>Akutsu, T., J. Saito, R. Imai, T. Suzuki, and X. D. Cao. Dynamic particle image velocimetry study of the aortic flow field of contemporary mechanical bileaflet prostheses. *J. Artif. Organs* 11:75–90, 2008.
- <sup>3</sup>Bellhouse, B. J., and F. H. Bellhouse. Mechanism of closure of the aortic valve. *Nature* 217:86–87, 1968.
- <sup>4</sup>Belz, G. G. Elastic properties and Windkessel function of the human aorta. *Cardiovasc. Drugs Ther.* 9(1):73–83, 1995.
- <sup>5</sup>Burgmann, S., S. Große, W. Schröder, J. Roggenkamp, S. Jansen, and F. Gräf. A refractive index-matched facility for fluid–structure interaction studies of pulsatile and oscillating flow in elastic vessels of adjustable compliance. *Exp. Fluids* 47:865–881, 2009.
- <sup>6</sup>Fukuda, I., S. Fujimori, K. Daitoku, H. Yanaoka, and T. Inamura. Flow velocity and turbulence in the transverse aorta of a proximally directed aortic cannula: hydrodynamic study in a transparent model. *Ann. Thorac. Surg.* 87:1866–1871, 2009.
- <sup>7</sup>Geoghegan, P. H., N. A. Buchmann, C. J. T. Spence, S. Moore, and M. Jermy. Fabrication of rigid and flexible refractive-index-matched flow phantoms for flow visualization and optical flow measurements. *Exp. Fluids* 52(5):1331–1347, 2012.
- <sup>8</sup>Glasser, S. P., D. K. Arnett, G. E. McVeigh, S. M. Finkelstein, A. J. Bank, D. J. Morgan, and J. N. Cohn. Vascular compliance and cardiovascular disease: a risk factor or a marker? *Am. J. Hypertens.* 10:1175–1189, 1997.
- <sup>9</sup>Gülan, U., B. Lüthi, M. Holzner, A. Liberzon, A. Tsinobor, and W. Kinzelbach. Experimental study of aortic flow in the ascending aorta via particle tracking velocimetry. *Exp. Fluids* 53(5):1469–1485, 2012.
- <sup>10</sup>Gülan, U., B. Lüthi, M. Holzner, A. Liberzon, A. Tsinobor, and W. Kinzelbach. Experimental investigation of the influence of the aortic stiffness on hemodynamics in the ascending aorta. *IEEE J. Biomed. Health Inform.* 18(6):1775–1780, 2014.
- <sup>11</sup>Hall, J. E., and A. C. Guyton. *Guyton and Hall Textbook of Medical Physiology*. Philadelphia: W. B. Saunders Company, 2000.
- <sup>12</sup>Hirata, K., F. Triposkiadis, E. Sparks, J. Bowen, C. F. Wooley, and H. Boudoulas. The Marfan syndrome: abnormal aortic elastic properties. *J. Am. Coll. Cardiol.* 18:57–63, 1991.

- <sup>13</sup>Kelly, R. P., R. Tunin, and D. A. Kass. Effect of reduced aortic compliance on cardiac efficiency and contractile function of in situ canine left ventricle. *Circ. Res.* 71:490–502, 1992.
- <sup>14</sup>Keshavarz-Motamed, Z., E. R. Edelman, P. K. Motamed, J. Garcia, J. N. Dahdah, and L. Kadem. The role of aortic compliance in determination of coarctation severity: lumped parameter modeling, in vitro study and clinical evaluation. *J. Biomech.* 48(16):4229–4237, 2015.
- <sup>15</sup>Keshavarz-Motamed, Z., J. Garcia, N. Maftoon, E. Bardard, P. Chetaille, and L. Kadem. A new approach for the evaluation of the severity of coarctation of the aorta using Doppler velocity index and effective orifice area: in vitro validation and clinical implications. *J. Biomech.* 45(7):1239–1245, 2012.
- <sup>16</sup>Laogun, A. A., and R. G. Gosling. In vivo arterial compliance in man. *Clin. Phys. Physiol. Meas.* 3:201–2012, 1982.
- <sup>17</sup>Liepsch, D., S. Moravec, and R. Baumgart. Some flow visualization and laser-Doppler-velocity measurements in a true-to-scale elastic model of a human aortic arch, a new model technique. *Biorheology* 29(5–6):563–580, 1992.
- <sup>18</sup>Lund-Johansen, P. The hemodynamics of the aging cardiovascular system. *J. Cardiovasc. Pharmacol.* 12:20–30, 1988.
- <sup>19</sup>Madhavan, S., W. L. Ooi, H. Cohen, and M. H. Alderman. Relation of pulse pressure and blood pressure reduction to the incidence of myocardial infarction. *Hypertension* 23:395–401, 1994.
- <sup>20</sup>Nguyen, T. T., R. Mongrain, J. Brunette, J. C. Tardif, and O. F. Bertrand. Method for matching the refractive index and kinematic viscosity of a blood analog for flow visualization in hydraulic cardiovascular models. *J. Biomech. Eng.* 126:529–536, 2004.
- <sup>21</sup>O'Rourke, M. F., A. P. Avolio, and W. W. Nichols. Left ventricular-systemic arterial coupling in humans and strategies to improve coupling in disease states. In: *Ventricular-Vascular Coupling*, edited by F. C. P. Yin. New York: Springer, 1987, pp. 1–19.
- <sup>22</sup>O'Rourke, M. F., J. A. Staessen, C. Vlachopoulos, D. Duprez, and G. E. Plante. Clinical applications of arterial stiffness; definitions and reference values. *Am. J. Hypertens.* 15:426–444, 2002.
- <sup>23</sup>Pielhop, K., C. Schmidt, S. Zholtovski, M. Klaas, and W. Schröder. Experimental investigation of the flow field in an elastic 180° curved vessel. *Exp. Fluids* 55:1816, 2014.
- <sup>24</sup>Raffel, M., C. S. Willert, S. Wereley, and J. Kompenhans. *Particle Image Velocimetry: A practical guide*. Berlin: Springer, 2007.
- <sup>25</sup>Stoiber, M., T. Schlöglhofer, P. Aigner, C. Grasl, and H. Schima. An alternative method to create highly transparent hollow models for flow visualization. *Int. J. Artif. Organs* 36(2):131–134, 2013.
- <sup>26</sup>Yip, R., R. Mongrain, A. Ranga, J. Brunette, and R. Cartier. Development of anatomically correct mock-ups of the aorta for PIV investigations. In: *Proceedings of the Canadian Engineering Education Association*, 2004.